

## Research Article

# Modeling of Optical Nanoantennas

**Bedir B. Yousif<sup>1</sup> and Ahmed S. Samra<sup>2</sup>**

<sup>1</sup> *Electrical Engineering Department, Faculty of Engineering, Kafrelsheikh University, Kafrelsheikh 35514, Egypt*

<sup>2</sup> *Electronics and Communications Department, Faculty of Engineering, Mansoura University, Mansoura 35516, Egypt*

Correspondence should be addressed to Bedir B. Yousif, bedir.yousif@gmail.com

Received 11 May 2012; Accepted 3 October 2012

Academic Editor: Sergi Gallego

Copyright © 2012 B. B. Yousif and A. S. Samra. This is an open access article distributed under the Creative Commons Attribution License, which permits unrestricted use, distribution, and reproduction in any medium, provided the original work is properly cited.

The optical properties of plasmonic nanoantennas are investigated in detail using the finite integration technique (FIT). The validity of this technique is verified by comparison to the exact solution generalized Mie method (GMM). The influence of the geometrical parameters (antenna length, gap dimension, and shapes) on the antenna field enhancement and spectral response is discussed. Localized surface plasmon resonances of Au (gold) dimers nanospheres, bowtie, and aperture bowtie nanoantennas are modeled. The enhanced field is equivalent to a strong light spot which can lead to the resolution improvement of the microscopy and optical lithography, thus increasing the optical data storage capacity. Furthermore, the sensitivity of the antennas to index changes of the environment and substrate is investigated in detail for biosensing applications. We confirm that our approach yields an exact correspondence with GMM theory for Au dimers nanospheres at gap dimensions 5 nm and 10 nm but gives an approximation error of less than 1.37% for gap dimensions 1 nm and 2 nm with diameters approaching 80 nm. In addition, the far-field characteristics of the aperture bowtie nanoantenna such as directivity and gain are studied. The promising results of this study may have useful potential applications in near-field sample detection, optical microscopy, and so forth.

## 1. Introduction

The study of optical phenomena related to the electromagnetic response of metals has been recently termed plasmonics or nanoplasmonics. This rapidly growing field of nanoscience is mostly concerned with the control of optical radiation on the subwavelength scale [1]. The interaction of light with metal nanostructures is hidden in the frequency dependence of the metal's complex dielectric function. Properly designed nanostructures are known to produce the so-called hot spots where the incident electromagnetic field is enhanced by several orders of magnitude. The plasmonic resonances observed in such structures open the possibility to build antennas operating in the visible [2, 3]. Their hot spots can be used to trigger nonlinear effects and to couple electromagnetic radiation efficiently between the antennas and dipole emitters. Experimental techniques such as tip-enhanced Raman spectroscopy or surface-enhanced Raman spectroscopy demonstrate the potential of such hot spots to detect radiative emitters with sensitivity down to a single molecule [4–10]. The enhancement of the fluorescence of molecules placed near a plasmonic nanostructure has been

observed recently, tuning the plasmon resonance either to the excitation or the emission of the molecules [11–14].

In recent years, a variety of schemes taking advantage of localized near fields generated by metallic nanoparticles have been proposed to use them as optical nanoantennas [2, 3, 15–22]. Optical antennas consisting of nanometer size metallic particle can be used to improve the size mismatch between the diffraction limited spot of the excitation light and fluorescent molecules that are much smaller than the excitation wavelength [19]. Optical antennas can produce very high near-field intensities when they are optically excited with a wavelength suitably matched to the antenna size due to their localized surface plasmon resonances [3]. Passive optical antennas were first demonstrated in the microwave regime by Grober and coworkers [23]. Also, mid-infrared (mid-IR) passive antennas [15] and bowtie antenna-based bolometers [24, 25] have been implemented.

Near-field enhancement generated by optical antennas is useful for surface-enhanced Raman spectroscopy (SERS) [4, 5, 18, 26]. Recently, metallic nanoparticles have been utilized in biosensing [27], cancer treatment [28], spectral imaging [29], solar applications [30], and near-field probes [31].

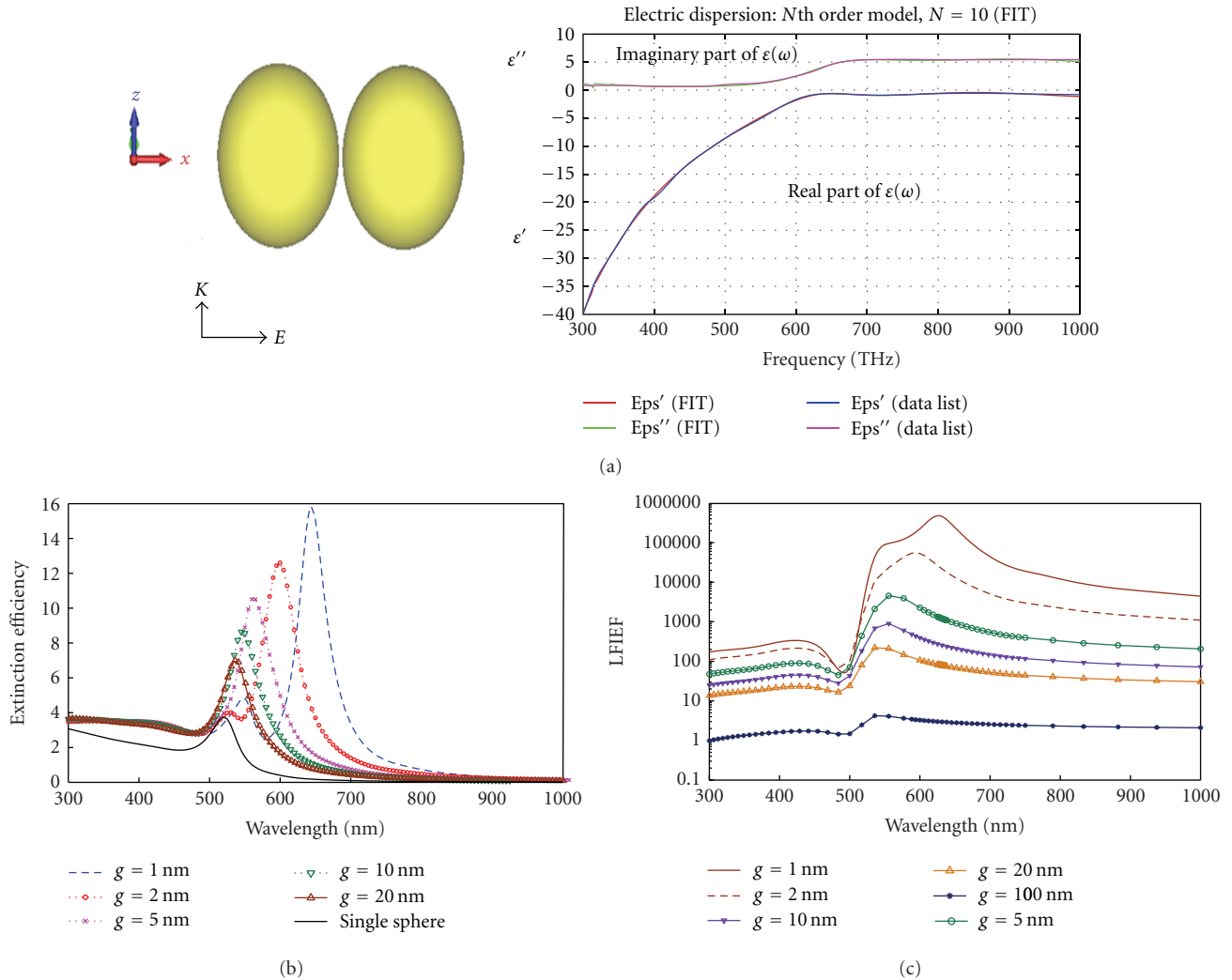


FIGURE 1: Simulation of gold dimer nanoantenna with FIT. (a) Schematic configuration of a gold dimer nanoantenna and its dielectric function  $\epsilon(\omega)$ . (b) Extinction coefficients for varying gaps as functions of incident wavelength. (c) The local field intensity enhancement factor (LFIEF) inside the gap ( $g$ ) of gold dimer nanoantenna.

Optical nanoantennas can also increase the excitation and emission rates of fluorescent molecules [11, 32]. The aim of this paper is to provide a detailed analysis and design of plasmonic nanoantennas for the near-field and spectral response enhancement.

The outline of this paper is as follows. Section 2 explains optical antenna design and modeling. Section 3 discusses the response of plasmonic nanoantennas with the validation of the results by comparison to the exact solution generalized Mie method (GMM) and the other published papers. Section 4 summarizes our observations and discuss potential future extensions of the research.

## 2. Optical Antenna Design and Modeling

The finite integration technique (FIT) using computer simulation technology (CST) microwave studio was used for the simulations to calculate the optical response of plasmonic nanoantennas. The microwave studio (MWS) developed

based on the FIT exhibits helpful functions especially suitable for simulating nanoantennas. It was adopted for modeling of monopole, dipole, bowtie, and nanooptical Yagi-Uda antennas [33–40]. The real and imaginary parts of the gold dielectric function are obtained from experimental data [41, 42]. The structures are illuminated from below, perpendicular to the antenna long axis. The gap between the nanostructure represents an essential feature of the antenna structure. To characterize the spectral response of the antenna and its intensity enhancement, we therefore calculate the field intensity inside this gap in relative units to the illumination intensity.

**2.1. Au Dimer Nanoantenna.** We first investigated plasmonic resonances and the local field intensity enhancement factor (LFIEF) inside the gap ( $g$ ) of dimer gold nanospheres as shown in Figure 1(a). A dimer formed by two identical spheres (with radius  $R = 40$  nm) of dielectric function  $\epsilon(\omega)$ , separated by a gap  $g$ , and embedded in a nonabsorbing

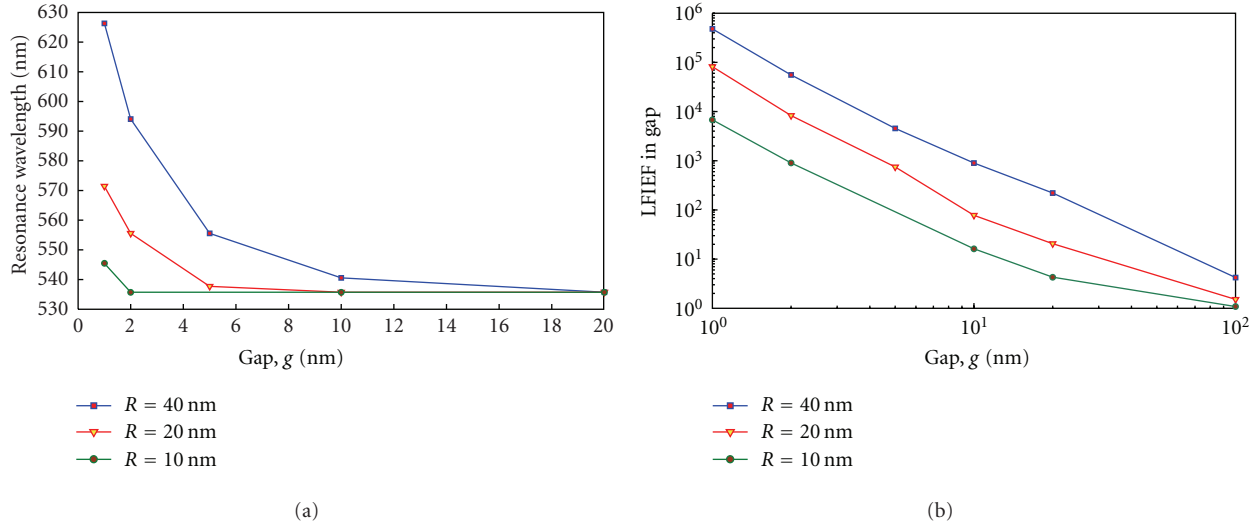


FIGURE 2: Gap dependence of the main coupled-LSPR. (a) Resonance wavelength and (b) LFIEF at the “hot spot” in the gap.

dielectric with  $\epsilon_M \approx 1$ ). The geometry of the antenna strongly influences its optical properties as indicated in Figures 1(b) and 1(c), which shows the calculated intensity spectra in the antenna gap of the dimer nanoantenna. In the spectral range of the calculation, the dimer nanoantenna at  $g = 1$  nm has two resonances at 540 nm and 635 nm as shown in Figure 1(b) extinction efficiency spectrum, where the field intensity (LFIEF) in the gap is about 100000 and 479200 times larger than the intensity of the illumination field as indicated in Figure 1(c). It is clear that the dimer gold spheres nanoantenna is essentially single mode for all gaps dimensions except only at  $g = 1$  nm, which has two modes due to the strong interaction coupling of the two nanospheres.

Stronger field enhancements can be achieved by decreasing the width of the gap and this is observed for the gap dimension 1 nm and the sphere diameter 80 nm in Figure 1(c). Note the presence of a dominant red-shifted localized surface plasmon resonance (LSPR) that moves further to the red for smaller gaps. Decreasing the gap width increases the antenna sensitivity as shown in Figure 2. We assume that this sensitivity is related to the spectral position of the antenna resonance at the maximum LFIEF. The main properties of the coupled-LSPR are characterized by its resonance wavelength and the LFIEF at the hot-spot (on the metal surface along the dimer axis in the gap). The gap dependence of these two quantities is summarized in Figures 2(a) and 2(b) for a gold dimer in air for different radius spheres ( $R = 40, 20,$  and  $10$  nm). It is worth stressing the fact that the resonance wavelength and the LFIEF at the hot-spot are plotted on semilog and log-log scales, respectively. A sharp change is seen for both for gap distances  $g$  below 20 nm. Actually, we can use this information as an “empirical” rule to establish in this case a characteristic distance beyond which the spheres can be considered as “independent.” Spheres can be effectively considered as electromagnetically independent if they are separated by more than 20 nm in the gap. For shorter distances, the interaction starts playing a role, and the main LSPR red

shifts with a concomitant steep increase in the hot-spot LFIEF at that wavelength. From Figure 2, it is also noted that decreasing the sphere radius decreases the antenna sensitivity and blue-shifted localized surface plasmon resonance (LSPR) that moves further.

Much more interesting is the antenna sensitivity to changes of the environmental index of refraction  $n_{env}$ . As shown in Figure 3 the spectral positions of the dipole resonances strongly depend on  $n_{env}$ . Increasing the refractive index of surrounding medium increases the antenna sensitivity and red-shifted localized surface plasmon resonance (LSPR) that moves further. Figure 3(b) shows a linear increase of the resonance wavelength for increasing  $n_{env}$  for different gap widths. The sensitivity is related to the spectral position of the antenna resonance. The further the resonance wavelength is shifted to the red, the higher the antenna sensitivity on index changes.

This section explains the effects of the polarization direction of the incident light on the optical properties of a gold dimer nanoantenna. By keeping the wave propagating in the  $z$ -direction, two cases with the polarization directions in the  $x$ - and  $y$ -directions are carefully considered. That is, the light is incident upon the antenna from the bottom side. The results are shown in Figure 4, where  $E_x$  and  $E_y$  polarizations are for Figures 4(a) and 4(b), respectively.

The light intensity is calculated and recorded at the origin in the middle of the dimer, through our interested optical region. It is found that both cases show a resonant behavior varying with wavelength in the light intensity’s spectra. Single resonance occurs in the optical range in both cases of polarization while two resonances appear in the visible light range at 555.56 nm for  $x$ -polarization and 517.24 nm for  $y$ -polarization. This can be explained by the strong interaction between the nanoantenna and the light through plasmon resonance when light polarized in  $x$ -direction. However, the variation magnitudes of  $E_x$  polarization (900.12) in Figure 4(a) are much larger than those of  $E_y$  polarization (0.831) in Figure 4(b). On the other hand, it can be

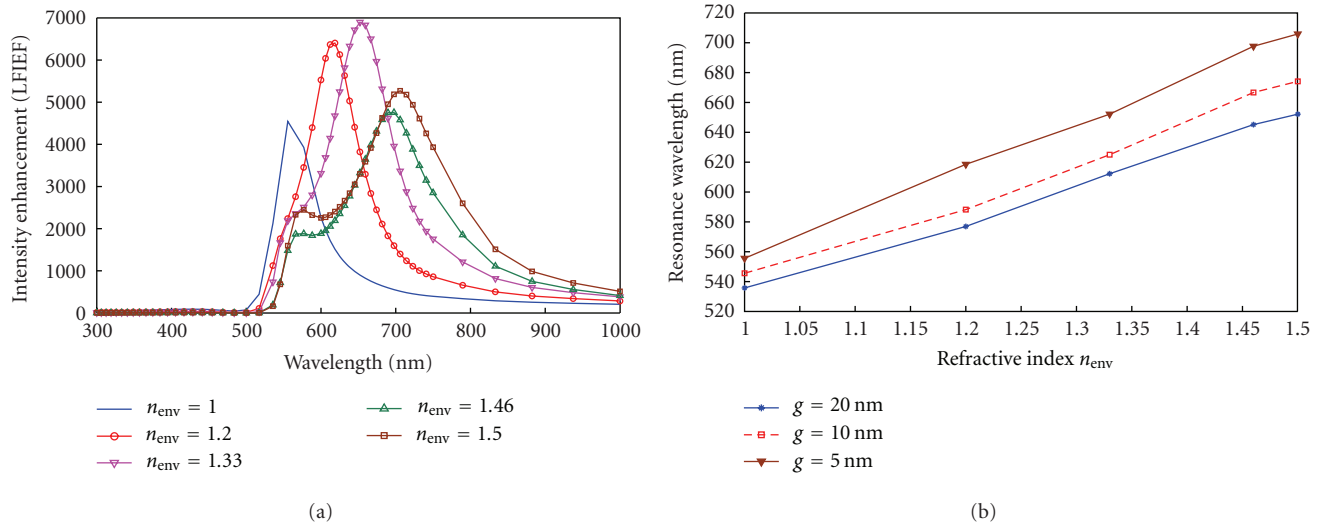


FIGURE 3: (a) Relative field intensity enhancement in the gap for a gold dimer nanoantenna with diameter 80 nm and gap width 5 nm as a function of the illumination wavelength for different refractive indexes  $n_{env}$  is used for the cover material. (b) Sensitivity of a gold dimer nanoantenna with sphere diameter 80 nm and various gap widths as a function of the environment index  $n_{env}$ .

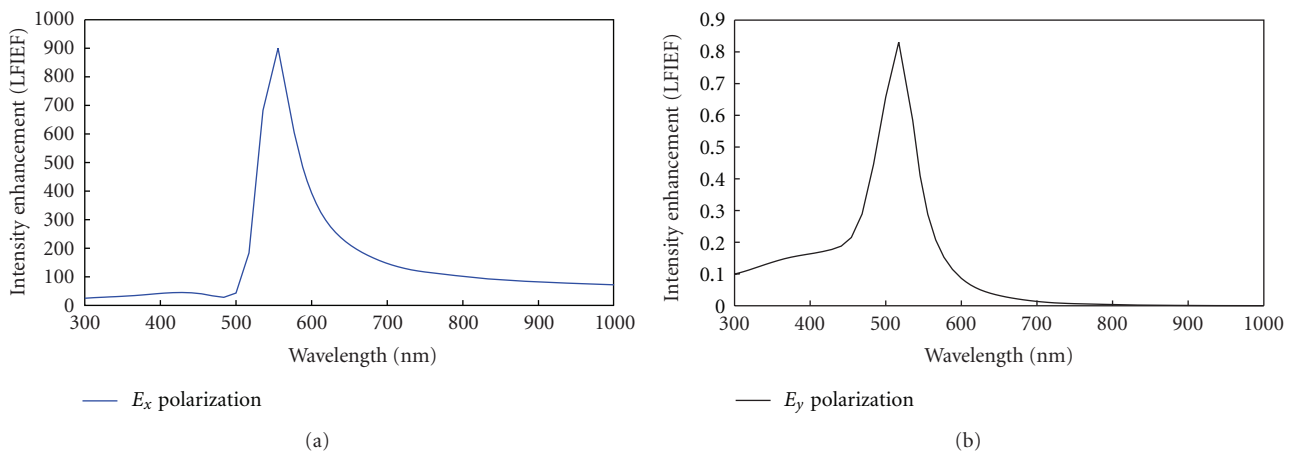


FIGURE 4: Light intensity as a function of incident wavelength for gold dimer nanoantenna with 80 nm sphere diameter and 10 nm gap width in air under different excitations.  $E_x$  polarization in (a) and  $E_y$  polarization in (b).

observed from the Figure 4 that the polarization is able to achieve much higher light intensity than the polarization at corresponding wavelengths. The reason is that for the coupling between two nanoparticles, a polarization along the longitudinal direction connecting them is preferable for a dipole-like excitation.

At microwave or radio frequencies, the substrate index  $n_s$  has a strong influence on the resonance spectrum of the antenna [43]. This dependence is in general used to design small antennas with dimensions well below the half wavelength condition. The same effect can be observed in Figure 5 for optical resonant antennas: an increasing substrate index leads to a red shift of the antenna resonance. At optical frequencies the antenna dimensions are as small as a few tens of nanometers, that is, below the half wavelength condition [44] and at the limit of today's fabrication techniques. Hence, designing smaller antennas by using high-index materials as substrate does not seem to be of great practical interest

presently. From Figure 5 it is clear that at  $n_s$  equal to 2.5 or 3 the response of the nanoantenna transfers from single mode to double mode, and this is similar or equivalent to increases in the size of the nanoantenna as stated above. The direction of propagation is also investigated with the effect of the substrate for a gold dimer with sphere diameter 80 nm and gap width 5 nm in air. The field enhancements which obtained in  $+z$  direction are much stronger than those of  $-z$  direction as shown in Figure 6. This is due to the strong interaction between the SPR in metallic nanoparticles and the substrate when the light incident from the bottom of substrate, in contrary when light illuminated from above where SPR is little or weakly interact with light as illustrated in Figure 6.

2.2. Au Bowtie and Bowtie Aperture Nanoantennas. Another way of increasing the near fields is to engineer the antenna

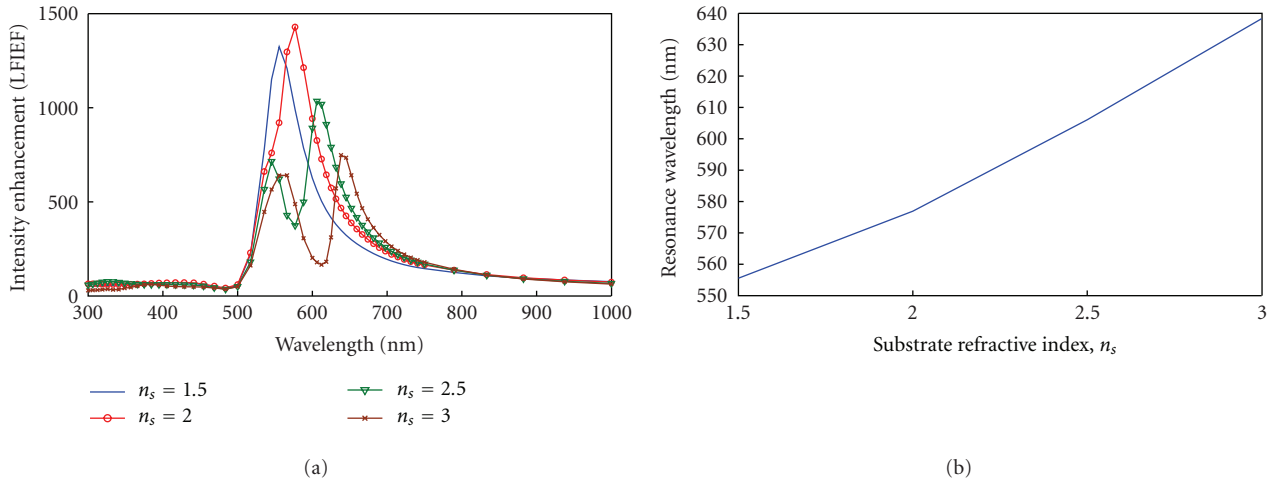


FIGURE 5: (a) Relative field intensity enhancement in the gap for a gold dimer nanoantenna with diameter 80 nm and gap width 10 nm as a function of the illumination wavelength for different refractive indexes  $n_s$  of substrate. (b) Sensitivity of nanoantenna as a function of the refractive indexes  $n_s$  of substrate.

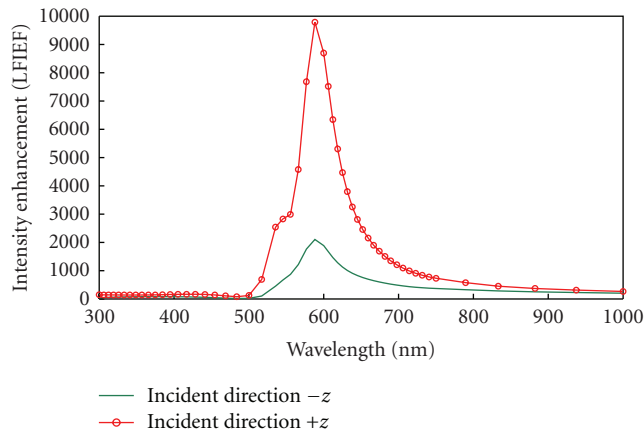


FIGURE 6: Relative field intensity enhancement in the gap for a gold dimer nanoantenna with diameter 80 nm and gap width 5 nm as a function of the illumination wavelength for wavevector  $k$  in  $-z$  and  $+z$  directions.

terminations and shapes. Bowtie optical antenna was also proven to be effective in reaching the spatial resolution well below the diffraction limit [23]. Similarly, metallic apertures like C-shaped aperture were also investigated because they can prove high transmission [45]. Moreover, the enhanced field via the strong light spot produced by the nanoantenna is highly dependent on its structure. Thus, considerable investigations were carried out based on different structural designs ranging from single nanoparticles of various shapes [46, 47] to delicately arranged nanoparticles including pairs and arrays [16, 48]. Bowtie antennas, namely, a pair of coupled triangular gold particles, offer higher near-field enhancements and better spatial confinement. When two triangular particles are placed side by side with the apices facing one another, the capacitive coupling between them will generate even higher fields than those generated by an isolated particle. Another typical design of the nanoparticle

pairs with good field confinement is the aperture bowtie nanoantenna. It was successfully fabricated in experiment, and there were wide studies exploring its controllable geometric effects on its optical properties, such as length and gap effects [16]. These studies are meaningful because bowtie nanoantenna has tunable characteristics. Bowtie-shaped aperture nanoantenna also attracts our recent research interests. Researchers have found that bowtie-shaped aperture can offer higher optical transmission than other apertures with regular shapes under the same resolution [49]. But recent studies provide little information about either its near-field resonant properties within a continuous wideband frequency spectrum or its far-field antenna performance. Such information is, however, quite important for optical communications. Therefore, it is worthwhile to extend both theoretical and experimental studies.

Here, we first clear that the near-field enhancement using the coupled triangular particles (bowtie antenna) as a function of incident wavelength for gold bowtie nanoantenna. The antennas are illuminated by a plane wave polarized along the  $x$ -axis and the substrate refractive index is 1.46, same boundary conditions as the above sections. The near-field response curve for the bowtie antenna is shown in Figure 7. When two triangular particles are placed side by side with the apices facing one another, the capacitive coupling between them will generate even higher fields than those generated by an isolated particle. Compared to the other antenna designs, bowties seem to offer the largest near-field enhancements and the smallest spatial extent for the field, that is, a single sharp optical spot. As shown in Figure 7, most of the electromagnetic energy is localized in the gap of the antenna. This property of bowties is crucial for applications requiring a very intense spatially confined optical spot.

In this section, both the near-field optical resonant properties and the far-field antenna characteristics are investigated for the bowtie shaped aperture nanoantenna. The nanoantenna consists of two fan-shaped hollow apertures

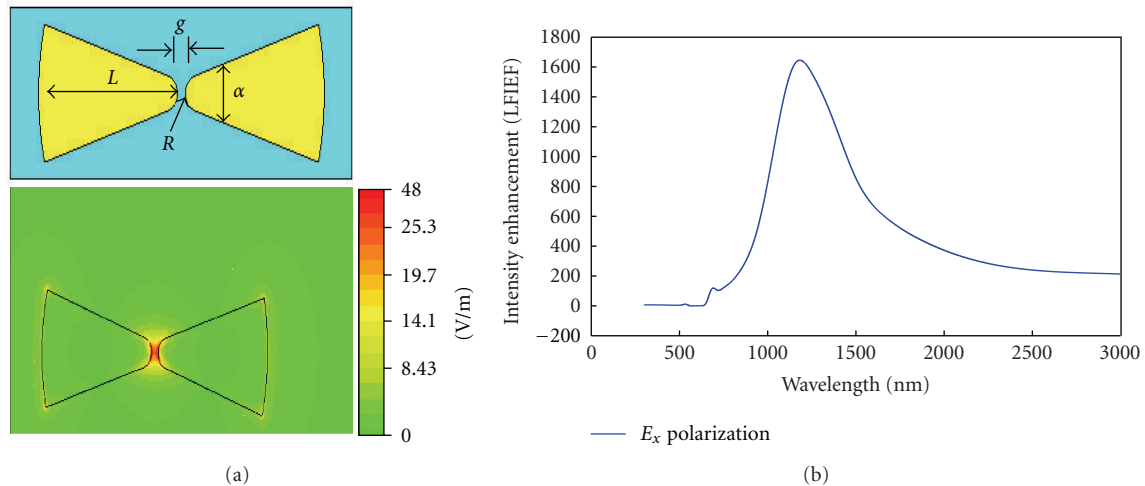


FIGURE 7: Near-field intensity distribution (a) around a triangular bowtie gold nanoantenna near the resonance wavelength (1363 nm) and (b) local field intensity enhancement in the middle of the gap with  $L = 240$  nm, gap of 20 nm, tip radius 20 nm, flare angle  $30^\circ$ , and  $n_s = 1.46$ .

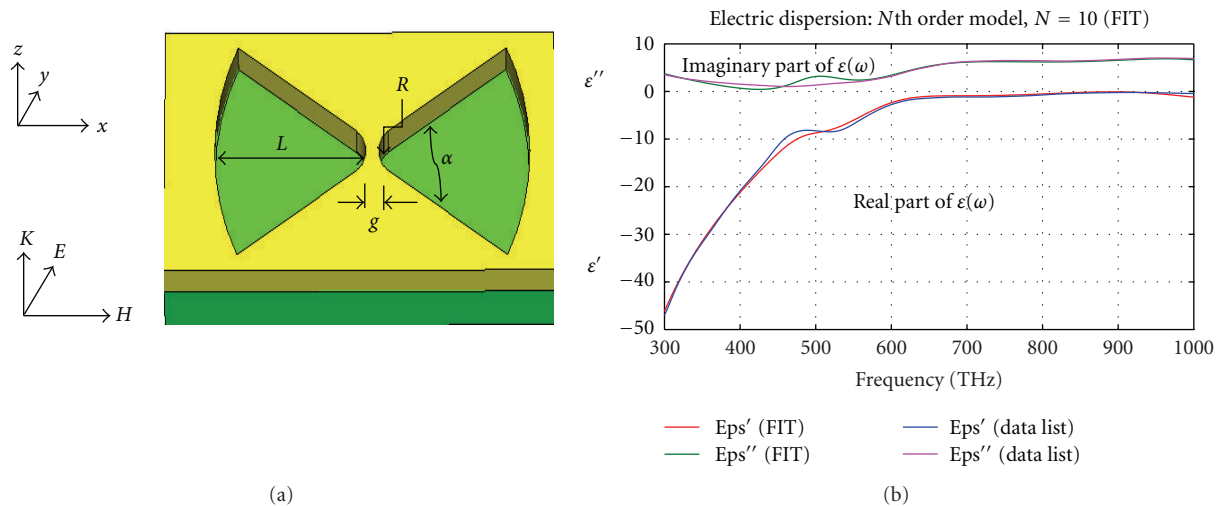


FIGURE 8: Simulation of bowtie shaped aperture nanoantenna with FIT. (a) Schematic configuration of bowtie aperture nanoantenna and its dielectric function  $\epsilon(\omega)$ .

mounted on a gold thin film. Configurations under consideration are depicted in Figure 8. Two tip-to-tip placed fan-shaped nanoapertures are mounted onto the gold thin film. Each has a length of 240 nm and a gap of 20 nm. The fan shape is more preferable than a triangle shape because it avoids the sharp corner which can cause undesirable singularity issues in design and because it is difficult to have its fabrication of high precision. Due to the same reasons, the tip of each fan-shaped aperture is rounded off with a radius of curve. Such a gold bowtie aperture nanoantenna is mount-integrated on the top of a substrate of silicon dioxide with a refractive index of 1.46. The nanoantenna with finite substrate is surrounded by the air. The coordinates in the figure are schematic and its origin is located in the middle of the nanoantenna. There are four geometric parameters of major concerns shown in Figure 8: length ( $L$ ), flare angle ( $\alpha$ ), radius of curve of each nanoaperture ( $R$ ), and distance between the two nanoapertures ( $g$ ). These parameters can

be used to optimize their effects on the optical properties of nanoantennas.

The effects of the polarization direction of the incident light on the optical properties of a gold aperture nanoantenna. The results are shown in Figure 9, where  $E_x$  and  $E_y$  polarization are for Figures 9(a) and 9(b), respectively. It is found that both cases show a resonant behavior varying with wavelength in the light intensity's spectra. Single resonance occurs in the optical range in the case of  $x$ -polarization while two resonances appear in the near infrared range in the case of  $y$ -polarization. This can be explained by the strong interaction between the nanoantenna and the light through plasmon resonance. However, the variation magnitudes of  $E_x$  polarization in Figure 9(a) are much smaller than those of  $E_y$  polarization in Figure 9(b).

Figure 10 shows how the light intensity changes with different radii of curvature. For each change, the flare angle, length, and gap separation of the aperture nanoantenna

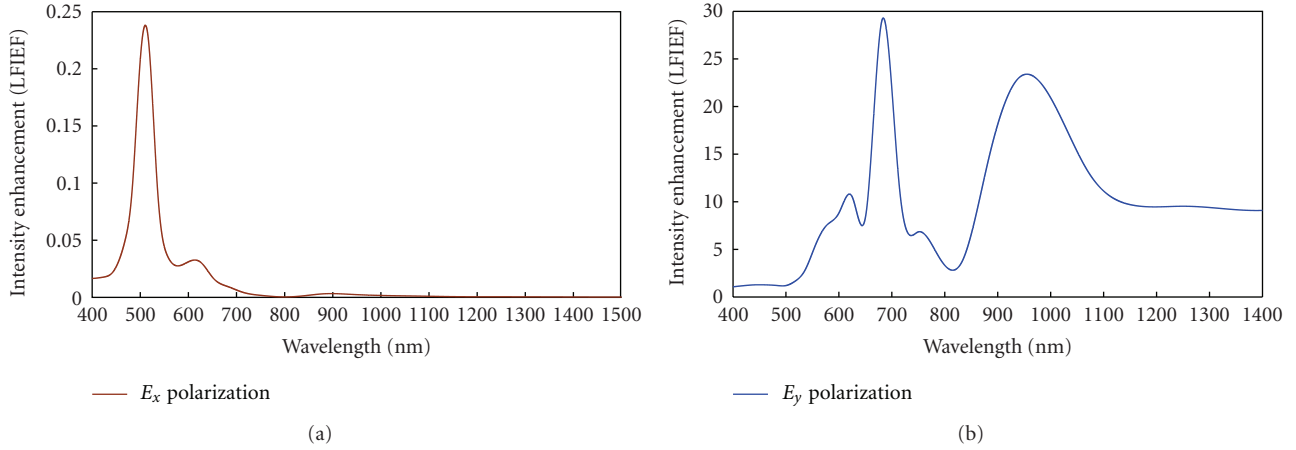


FIGURE 9: Light intensity as a function of incident wavelength for bowtie aperture nanoantenna different excitations.  $E_x$  polarization in (a) and  $E_y$  polarization in (b) at tip radius 30 nm, gap 20 nm, antenna length 240 nm, and flare angle  $60^\circ$ .

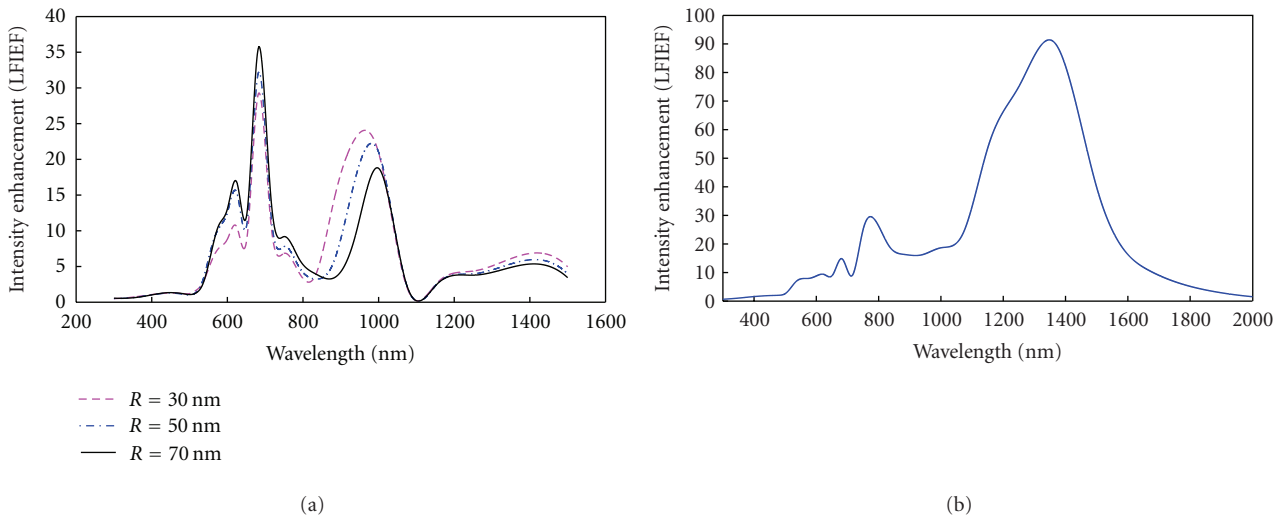


FIGURE 10: Light intensity enhancement as a function of incident wavelength for gold bowtie shaped aperture nanoantenna under different radii of curvature of nanoapertures.

are  $60^\circ$ , 240 nm, and 20 nm, respectively. From Figure 10, it can be observed that as  $R$  becomes smaller from 70 nm to 30 nm (i.e., the apex of the nanoaperture becomes sharper), the light intensity at both resonances turns higher at the second mode and the resonances move toward greater wavelength side, which means a red shift in the spectrum. As a result, if stronger enhancement is needed the bowtie aperture nanoantenna can be designed with appropriately sharper tip to meet such a requirement as shown in Figure 10(b), for the following design parameters  $R = 20$  nm,  $g = 20$  nm,  $\alpha = 30^\circ$ ,  $L = 240$  nm, and substrate refractive index  $= 1.46$ . From Figure 10(b), the stronger enhancement is observed and larger than in Figure 10(a) about three times.

In the far-field computation, the field patterns in the  $E$ -plane and  $H$ -plane of are plotted in Figures 11(a) and 11(b) for the bowtie-shaped aperture nanoantenna with a radius 30 nm of curvature and a flare angle of  $60^\circ$  at a wavelength of 500 nm (600 THZ). The patterns of the nanoantenna imply that a good directivity is achievable by the bowtie aperture.

From Figure 11, it is found that the half power bandwidths obtained are 37.5 and 54.1 in both planes, respectively. The following approximation formulation for a directional pattern is used [43]:

$$D_0 = \frac{41253}{(\Theta_{1d}\Theta_{2d})}, \tag{1}$$

where  $\Theta_{1d}$  and  $\Theta_{2d}$  stand for the half power bandwidths in degrees in two respective perpendicular planes. The directivity calculated is 20.334, equivalent to 13.1 dB. In the same fashion, the gain for antenna satisfies the following empirical equation [43]:

$$G_0 = \frac{30000}{(\Theta_{1d}\Theta_{2d})}. \tag{2}$$

From (2), the gain of nanoantenna calculated is 11.7 dB. It should be noted that the directivity is obtained by the formula based on some approximations. Equation (1)

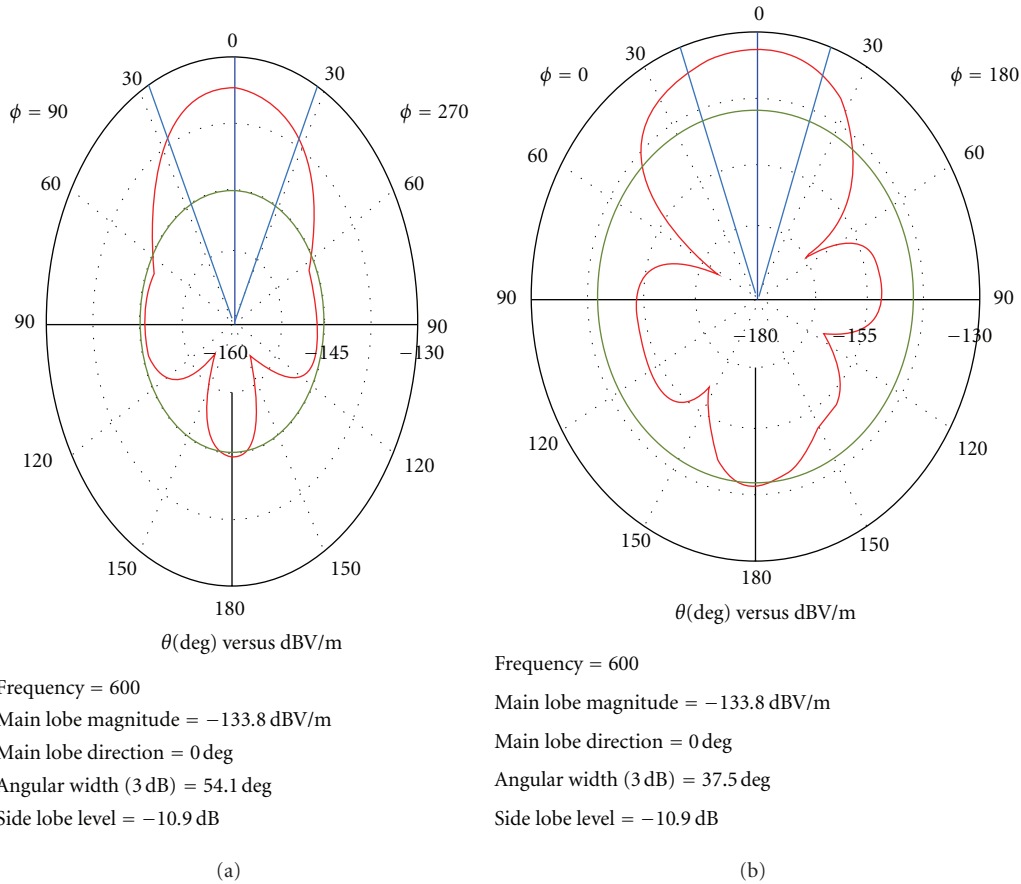


FIGURE 11: Field pattern of bowtie-shaped aperture nanoantenna. (a) *E*-plane. (b) *H*-plane (frequency in THZ).

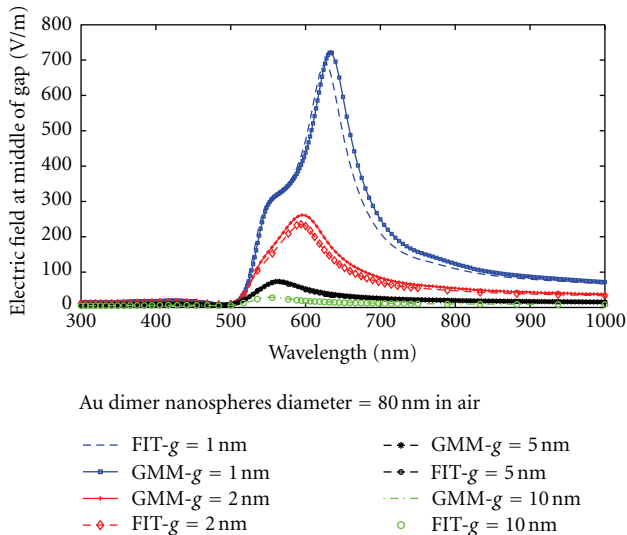


FIGURE 12: Comparison of electric field spectra calculated in middle of the gap using the FIT and GMM for various gaps of gold dimer nanoantenna in air.

suggests one narrow major lobe and very negligible minor lobes. Hence, it might be not adequately exact in our case with larger side lobes. Even so, the results could serve as a fair reference for nanoantenna designs.

### 3. Validity of FIT

As a numerical method, it is necessary to judge and review the validity of the FIT method before its application in optical nanoantenna. For this purpose, we performed FIT simulations for gold dimer nanospheres with diameter 80 nm in air surrounding medium and compared the results with exact solution generalized Mie method (GMM) [50–52] calculations for the same system. The results are shown in Figure 12, we observe an exact correspondence between the two models for the gaps width that are 5 nm and 10 nm, respectively. From Figure 12 at gap width 1 nm and nanospheres diameter 80 nm, the peak of electric field is 720 V/m as published in the papers [35, 53] and the resonance wavelength 634 nm.

### 4. Conclusion

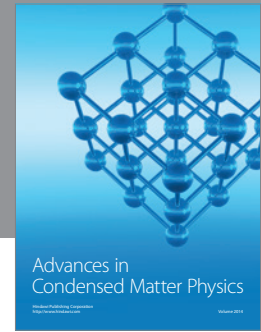
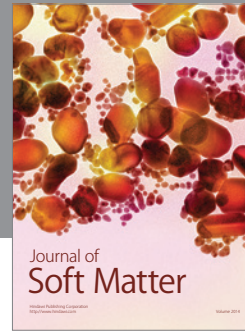
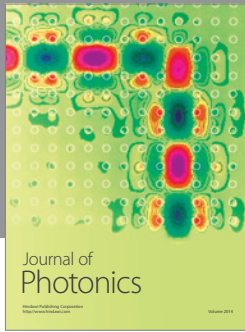
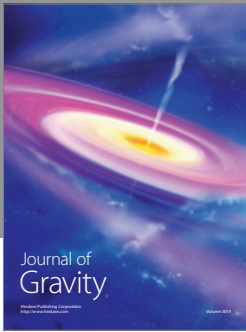
In this paper, we investigate plasmonic gold dimer bowtie and bowtie aperture nanoantennas, with particular emphasis on near-field resonances and far-field radiation properties. Such properties have been explored numerically in detail based on the FIT algorithm. It is found that this antenna can exhibit a resonant behavior in the optical and near-infrared regions. In addition, SPR resonances can occur at different positions, depending on the polarization directions of incident light, refractive index of surrounding medium,

substrate, and geometric parameters of the nanoantenna (length, gap width, and shapes). Polarization along antenna axis can give better efficiency of enhancement in dimer sphere and bowtie nanoantenna, in contrast to bowtie aperture nanoantenna, where the enhancement field occurred in the direction of minor axis of the antenna ( $y$ -polarization) as explained previously. Moreover, the field enhancement produced is related to the geometric parameters including the radius of nanospheres, tip radius, and the gap width between the nanoparticles. A nanoantenna with a smaller gap supports higher light intensity at resonance and red-shifts the resonances at the same time. The results of this paper should be useful for choosing the best suited antenna geometry for a given application.

## References

- [1] L. Novotny and B. Hecht, *Principles Of Nano-Optics*, Cambridge University Press, 1st edition, 2006.
- [2] D. P. Fromm, A. Sundaramurthy, P. James Schuck, G. Kino, and W. E. Moerner, "Gap-dependent optical coupling of single "bowtie" nanoantennas resonant in the visible," *Nano Letters*, vol. 4, no. 5, pp. 957–961, 2004.
- [3] P. Mühlischlegel, H. J. Eisler, O. J. F. Martin, B. Hecht, and D. W. Pohl, "Resonant optical antennas," *Science*, vol. 308, no. 5728, pp. 1607–1609, 2005.
- [4] S. Nie and S. R. Emory, "Probing single molecules and single nanoparticles by surface-enhanced Raman scattering," *Science*, vol. 275, no. 5303, pp. 1102–1106, 1997.
- [5] K. Kneipp, Y. Wang, H. Kneipp et al., "Single molecule detection using surface-enhanced Raman scattering (SERS)," *Physical Review Letters*, vol. 78, no. 9, pp. 1667–1670, 1997.
- [6] H. Xu, E. J. Bjerneld, M. Käll, and L. Börjesson, "Spectroscopy of single hemoglobin molecules by surface enhanced Raman scattering," *Physical Review Letters*, vol. 83, no. 21, pp. 4357–4360, 1999.
- [7] N. Félidj, J. Aubard, G. Lévi et al., "Optimized surface-enhanced Raman scattering on gold nanoparticle arrays," *Applied Physics Letters*, vol. 82, no. 18, pp. 3095–3097, 2003.
- [8] W. Zhang, X. Cui, B. S. Yeo, T. Schmid, C. Hafner, and R. Zenobi, "Nanoscale roughness on metal surfaces can increase tip-enhanced raman scattering by an order of magnitude," *Nano Letters*, vol. 7, no. 5, pp. 1401–1405, 2007.
- [9] L. Rogobete, F. Kaminski, M. Agio, and V. Sandoghdar, "Design of plasmonic nanoantennae for enhancing spontaneous emission," *Optics Letters*, vol. 32, no. 12, pp. 1623–1625, 2007.
- [10] T. H. Taminiau, F. D. Stefani, F. B. Segerink, and N. F. Van Hulst, "Optical antennas direct single-molecule emission," *Nature Photonics*, vol. 2, no. 4, pp. 234–237, 2008.
- [11] S. Kuhn, U. Hakanson, L. Rogobete, and V. Sandoghdar, "Enhancement of single-molecule fluorescence using a gold nanoparticle as an optical nanoantenna," *Physical Review Letters*, vol. 96, 4 pages, 2006.
- [12] T. H. Taminiau, R. J. Moerland, F. B. Segerink, L. Kuipers, and N. F. Van Hulst, " $\lambda/4$  resonance of an optical monopole antenna probed by single molecule fluorescence," *Nano Letters*, vol. 7, no. 1, pp. 28–33, 2007.
- [13] P. Bharadwaj and L. Novotny, "Spectral dependence of single molecule fluorescence enhancement," *Optics Express*, vol. 15, no. 21, pp. 14266–14274, 2007.
- [14] F. Tam, G. P. Goodrich, B. R. Johnson, and N. J. Halas, "Plasmonic enhancement of molecular fluorescence," *Nano Letters*, vol. 7, no. 2, pp. 496–501, 2007.
- [15] K. B. Crozier, A. Sundaramurthy, G. S. Kino, and C. F. Quate, "Optical antennas: resonators for local field enhancement," *Journal of Applied Physics*, vol. 94, no. 7, pp. 4632–4642, 2003.
- [16] A. Sundaramurthy, K. B. Crozier, G. S. Kino, D. P. Fromm, P. J. Schuck, and W. E. Moerner, "Field enhancement and gap-dependent resonance in a system of two opposing tip-to-tip Au nanotriangles," *Physical Review B*, vol. 72, no. 16, Article ID 165409, 6 pages, 2005.
- [17] A. Sundaramurthy, P. J. Schuck, N. R. Conley, D. P. Fromm, G. S. Kino, and W. E. Moerner, "Toward nanometer-scale optical photolithography: utilizing the near-field of bowtie optical nanoantennas," *Nano Letters*, vol. 6, no. 3, pp. 355–360, 2006.
- [18] D. P. Fromm, A. Sundaramurthy, A. Kinkhabwala, P. J. Schuck, G. S. Kino, and W. E. Moerner, "Exploring the chemical enhancement for surface-enhanced Raman scattering with Au bowtie nanoantennas," *The Journal of chemical physics*, vol. 124, no. 6, Article ID 061101, 4 pages, 2006.
- [19] P. J. Schuck, D. P. Fromm, A. Sundaramurthy, G. S. Kino, and W. E. Moerner, "Improving the mismatch between light and nanoscale objects with gold bowtie nanoantennas," *Physical Review Letters*, vol. 94, no. 1, Article ID 017402, 4 pages, 2005.
- [20] J. N. Farahani, D. W. Pohl, H. J. Eisler, and B. Hecht, "Single quantum dot coupled to a scanning optical antenna: a tunable superemitter," *Physical Review Letters*, vol. 95, no. 1, Article ID 017402, 4 pages, 2005.
- [21] J. N. Farahani, H. J. Eisler, D. W. Pohl et al., "Bow-tie optical antenna probes for single-emitter scanning near-field optical microscopy," *Nanotechnology*, vol. 18, no. 12, Article ID 125506, 2007.
- [22] B. Hecht, P. Mühlischlegel, J. N. Farahani et al., "Prospects of resonant optical antennas for nano-analysis," *Chimia*, vol. 60, no. 11, pp. A765–A769, 2006.
- [23] R. D. Grober, R. J. Schoelkopf, and D. E. Prober, "Optical antenna: towards a unity efficiency near-field optical probe," *Applied Physics Letters*, vol. 70, no. 11, pp. 1354–1356, 1997.
- [24] J. Alda, J. M. Rico-García, J. M. López-Alonso, and G. Boreman, "Optical antennas for nano-photon applications," *Nanotechnology*, vol. 16, no. 5, pp. S230–S234, 2005.
- [25] F. J. González, B. Ilic, J. Aida, and G. D. Boreman, "Antenna-coupled infrared detectors for imaging applications," *IEEE Journal on Selected Topics in Quantum Electronics*, vol. 11, no. 1, pp. 117–120, 2005.
- [26] K. Kneipp, H. Kneipp, I. Itzkan, R. R. Dasari, and M. S. Feld, "Ultrasensitive chemical analysis by Raman spectroscopy," *Chemical Reviews*, vol. 99, no. 10, pp. 2957–2975, 1999.
- [27] D. Enders, S. Rupp, A. Küller, and A. Pucci, "Surface enhanced infrared absorption on Au nanoparticle films deposited on SiO<sub>2</sub>/Si for optical biosensing: detection of the antibody-antigen reaction," *Surface Science*, vol. 600, no. 23, pp. L305–L308, 2006.
- [28] X. Huang, I. H. El-Sayed, W. Qian, and M. A. El-Sayed, "Cancer cells assemble and align gold nanorods conjugated to antibodies to produce highly enhanced, sharp, and polarized surface Raman spectra: a potential cancer diagnostic marker," *Nano Letters*, vol. 7, no. 6, pp. 1591–1597, 2007.
- [29] L. J. Steven, S. Ravikant, and C. Niloy, "Rapid spectral analysis for spectral imaging," *Biomedical Optics Express*, vol. 1, pp. 157–164, 2010.
- [30] S. Pillai, K. R. Catchpole, T. Trupke, G. Zhang, J. Zhao, and M. A. Green, "Enhanced emission from Si-based light-emitting

- diodes using surface plasmons,” *Applied Physics Letters*, vol. 88, Article ID 161102, 3 pages, 2006.
- [31] P. Anger, P. Bharadwaj, and L. Novotny, “Enhancement and quenching of single-molecule fluorescence,” *Physical Review Letters*, vol. 96, Article ID 113002, 4 pages, 2006.
- [32] M. Danckwerts and L. Novotny, “Optical frequency mixing at coupled gold nanoparticles,” *Physical Review Letters*, vol. 98, Article ID 026104, 4 pages, 2007.
- [33] Y. M. Wu, L. W. Li, and B. Liu, “Gold bow-tie shaped aperture nanoantenna: wide band near-field resonance and far-field radiation,” *IEEE Transactions on Magnetics*, vol. 46, no. 6, pp. 1918–1921, 2010.
- [34] K. J. Ooi, P. Bai, M. X. Gu, and L. K. Ang, “Design of a monopole-antenna-based resonant nanocavity for detection of optical power from hybrid plasmonic waveguides,” *Optics Express*, vol. 19, no. 18, pp. 17075–17085, 2011.
- [35] C. S. T. Microwave Studio, 2011, <http://www.cst.com/>.
- [36] E. Tatartschuk, E. Shamonina, and L. Solymar, “Plasmonic excitations in metallic nanoparticles: resonances, dispersion characteristics and near-field patterns,” *Optics Express*, vol. 17, no. 10, pp. 8447–8460, 2009.
- [37] T. H. Taminiau, F. B. Segerink, and N. F. van Hulst, “A monopole antenna at optical frequencies: single-molecule near-field measurements,” *IEEE Transactions on Antennas and Propagation*, vol. 55, no. 11 I, pp. 3010–3017, 2007.
- [38] A. E. Miroshnichenko, I. S. Maksymov, A. R. Davoyan, C. Simovski, P. Belov, and Y. S. Kivshar, “An arrayed nanoantenna for broadband light emission and detection,” *Physica Status Solidi*, vol. 5, no. 11 I, pp. 347–349, 2011.
- [39] T. Weiland, “A discretization method for the solution of maxwell’s equations for six-component fields,” *AEU-Archiv für Elektronik und Übertragungstechnik*, vol. 31, no. 3, pp. 116–120, 1977.
- [40] T. H. Taminiau, R. J. Moerland, F. B. Segerink, L. Kuipers, and N. F. Van Hulst, “Enhanced directional excitation and emission of single emitters by a nano-optical Yagi-Uda antenna,” *Optics Express*, vol. 16, no. 14, pp. 16858–16866, 2008.
- [41] P. B. Johnson and R. W. Christy, “Optical constants of the noble metals,” *Physical Review B*, vol. 6, Article ID 4370, 1972.
- [42] E. Palik, *Handbook of Optical Constants of Solids*, vol. 1, Academic, New York, NY, USA, 1985.
- [43] C. A. Balanis, *Antenna Theory: Analysis and Design*, Wiley-Interscience, Hoboken, NJ, USA, 2005.
- [44] L. Novotny, “Effective wavelength scaling for optical antennas,” *Physical Review Letters*, vol. 98, Article ID 266802, 4 pages, 2007.
- [45] X. Shi, L. Hesselink, and R. L. Thornton, “Ultrahigh light transmission through a C-shaped nanoaperture,” *Optics Letters*, vol. 28, no. 15, pp. 1320–1322, 2003.
- [46] C. Li, G. W. Kattawar, P. W. Zhai, and P. Yang, “Electric and magnetic energy density distributions inside and outside dielectric particles illuminated by a plane electromagnetic wave,” *Optics Express*, vol. 13, no. 12, pp. 4554–4559, 2005.
- [47] Z. Chen, X. Li, A. Taflove, and V. Backman, “Backscattering enhancement of light by nanoparticles positioned in localized optical intensity peaks,” *Applied Optics*, vol. 45, no. 4, pp. 633–638, 2006.
- [48] D. A. Genov, A. K. Sarychev, V. M. Shalaev, and A. Wei, “Resonant Field Enhancements from Metal Nanoparticle Arrays,” *Nano Letters*, vol. 4, no. 1, pp. 153–158, 2004.
- [49] L. Wang, S. M. Uppuluri, E. X. Jin, and X. Xu, “Nanolithography using high transmission nanoscale bowtie apertures,” *Nano Letters*, vol. 6, no. 3, pp. 361–364, 2006.
- [50] A. Bek, R. Jansen, M. Ringler, S. Mayilo, T. A. Klar, and J. Feldmann, “Fluorescence enhancement in hot spots of AFM-designed gold nanoparticle sandwiches,” *Nano Letters*, vol. 8, no. 2, pp. 485–490, 2008.
- [51] M. Ringler, A. Schwemer, M. Wunderlich et al., “Shaping emission spectra of fluorescent molecules with single plasmonic nanoresonators,” *Physical Review Letters*, vol. 100, no. 20, Article ID 203002, 2008.
- [52] L. Liu, B. Wang, X. Cao, X. Xu, and Y. Wang, “Comparison investigation of near- and far-field properties for plasmon resonance of silver nanosphere dimers,” *Photonics and Nanostructures*, vol. 10, no. 1, pp. 16–24, 2011.
- [53] J. Hoffman, C. Hafner, P. Leidenberger, J. Hesselbarth, and S. Burger, “Comparison of electromagnetic field solvers for the 3D analysis of plasmonic nano antennas,” in *Modeling Aspects in Optical Metrology II*, vol. 7390 of *Proceedings of the SPIE*, 2009.



**Hindawi**

Submit your manuscripts at  
<http://www.hindawi.com>

